Direct and Indirect Adaptive Inverse Control Design for Non-Minimum Phase EHA System with Periodic Disturbance via FASS-NLMS Algorithm

Rodrigo Possidônio Noronha *

* *Av. Newton Belo, S/N - Vila Maria, Imperatriz, CEP: 65906-335, Federal Institute of Maranhão, MA, (e-mail: rodrigo.noronha@ifma.edu.br)*

Abstract: In this paper, is performed the comparative analysis of performance between the direct and indirect adaptive inverse control applied to a non-minimum phase Electro-Hydraulic (EHA) system in the presence of a periodic disturbance signal. The performance of an adaptive inverse controller is influenced by the trade-off between the convergence speed and the steady-state Mean Square Error (MSE) during the update of the estimate of the weights vector. Aiming to propose a new optimization algorithm based on stochastic gradient descent, in this paper, a new version of Normalized Leat Mean Square (NLMS) algorithm with adaptive step size is proposed, with the objective of obtaining a good trade-off between convergence speed and the steady-state MSE. For this, the step size is adapted by a Mamdani Fuzzy Inference System (MFIS) as a function of the squared error and of the normalized time instant by the Min-Max method. Computational results illustrate the efficiency of the proposed optimization algorithm in the design of these two approaches of adaptive inverse control.

Keywords: Adaptive Filter; Adaptive Inverse Control; Fuzzy Systems; NLMS; Stochastic Gradient Descent.

1. INTRODUCTION

At the First IFAC Workshop in Control and Signal Processing in San Francisco, was proposed by Widrow and Walach (1983) the Adaptive Inverse Control (AIC) technique. The AIC is a control technique that deals with solving adaptive control theory problems using the adaptive filter theory. The objective of AIC is to obtain a controller that is equal to the plant inverse model, such that it is possible to control, without feedback, the plant dynamic and reject disturbances. The Direct Adaptive Inverse Control (DAIC) (Shafiq et al., 2014) and the Indirect Adaptive Inverse Control (IAIC) (Widrow and Walach, 2008) are two techniques of AIC, that possess a disturbance rejection ability due being implemented in a feedforward configuration (Shafiq et al., 2017). Some contributions to the IAIC and DAIC published in the literature can be found at Shafiq (2016); Kamanditya and Kusumoputro (2020); Zhang et al. (2018).

Even in the face of this similar characteristic, due to difference in the configuration for update the estimate of the weights vector of the controller, the DAIC and IAIC possess different performances in the tracking of the plant inverse dynamic and, consequently, of the reference signal. The weights vector of a DAIC and IAIC is updated through the minimization of a given performance index described as a function of the error used to update the estimate of the weights vector. Due to this, in the literature some proposals for the DAIC and IAIC design via optimization algorithms based on stochastic gradient descent can be found using the following algorithms: Least Mean Square (LMS) (Wang et al., 2013) and Normalized Least Mean Square (NLMS) (Shafiq et al., 2017; Ghazali et al., 2015). In this paper, only the NLMS algorithm is discussed for the DAIC and IAIC design, since this algorithm is less sensitive to variations in the input signal power and performs well on correlated signals (Benesty et al., 2006).

The choice of step size is important for a good performance of NLMS algorithm (Farhang-Boroujeny, 2013), since if the step size is large, the convergence speed of NLMS algorithm will be fast, but the steady-state Mean Square Error (MSE) will be large; if the step size is small, the convergence speed of NLMS algorithm will be slow, but the steady-state MSE will be small (Pauline et al., 2020). These characteristics are independent of the problem nature to be optimized (Bershad and Bermudez, 2020). According to Benesty et al. (2006), a good trade-off between the convergence speed and steady-state MSE is obtained through the adjust of the step size at each time instant. Thus, the adjust of the step size is fundamental for a good performance in the tracking of the plant inverse dynamic and, consequently, of the reference signal by the DAIC and IAIC.

In the literature, it is possible to find several methodologies that propose strategies to make the variable step size in order to obtain a good trade-off. Generally, these methodologies propose that during the first time instants the step size is large, and with the end of the time instants, the step

size is small (Pauline et al., 2020; Resende et al., 2018; Kim et al., 2020). On the other hand, in order for the methodologies to adjust the step size, additional information are required, such as damping factor, conditioning parameters, and others. In some cases, these methodologies require the use of high-order statistical measures, which are not always available in the context of real-time operation. Another problem, is to establish criteria so that the NLMS algorithm does not become unstable.

Through an MFIS, problems of various nature and difficult mathematical formulation can be solved (Li et al., 2019; Dhimish et al., 2018). Using an MFIS, it is possible to develop a fuzzy rule base based on the expert's knowledge to adapt the step size, independent, for example, of high-order statistical measurements. However, in the literature, to the present moment, there are few versions of NLMS algorithm with the adaptation of the step size performed by an MFIS. In Ng et al. (2009), for application in communication channel equalization, it was proposed to use an MFIS to adapt the step size as a function of the squared error. Thus, aiming to propose a new version of NLMS algorithm with the variable step size, in this paper it is proposed the Fuzzy Adaptive Step Size - Normalized Least Mean Square (FASS-NLMS) algorithm, in order to obtain a good trade-off between the convergence speed and the steady-state MSE. In the FASS-NLMS algorithm, the step size is adjusted by an MFIS, such that the step size is adapted, at each time instant, as a function of the squared error and of the normalized time instant by the Min-Max method.

The justification for using, in addition to the squared error, the normalized time instant as another input of the MFIS, is due to the instant be an important parameter for the convergence of the weights vector, since it is expected that at the end of the time instants occurs its convergence. For validation of the proposed optimization methodology, was performed the IAIC and DAIC design applied to a non-minimum phase plant referring to an Electro-Hydraulic Actuator system (EHA) in the presence of a periodic disturbance signal added to the control signal. The objective of performing the DAIC and IAIC design in this paper, is to compare the performance of these controllers, in the presence of a periodic disturbance signal, when the step size of NLMS algorithm is adapted by an MFIS. Until the present moment, according to the bibliographic studies carried out by the author, no paper has been published in the literature proposing the use of an NLMS algorithm with the step size adapted by an MFIS used for the IAIC and DAIC design and performed the performance comparison in the presence of a periodic disturbance signal. Thus, the contribution proposed in this paper is clear and justified. This paper is organized as follows: in Section 2, the mathematical formulations for the IAIC are presented; in Section 3, the mathematical formulations for the DAIC are presented; in Section 4, the methodology for adaptation of the step size using a MFIS is presented; in Section 5, the results obtained by the applying DAIC to a non-minimum phase plant in the presence of a periodic disturbance signal added to the control signal are presented.

2. INDIRECT ADAPTIVE INVERSE CONTROL

Let the relationship between the control signal $u(k)$ and output signal $y(k)$ of a discrete-time stable or stabilizable plant be given by:

$$y(k) = q^{-d}\frac{B(q^{-1})}{A(q^{-1})}u(k) = P(q^{-1})u(k), \qquad (1)$$

where $P(q^{-1})$ is the plant model, $A(q^{-1}) = 1 + a_1q^{-1} + a_2q^{-2} + \ldots + a_nq^{-n}$, $B(q^{-1}) = 1 + b_1q^{-1} + b_2q^{-2} + \ldots + b_mq^{-m}$. The operator q^{-1} is a delay operator such that $q^{-1}u(k) = u(k-1)$, $k \in \mathbb{N}$ is the time instant, $d \in \mathbb{N}$ is the delay between the control signal $u(k)$ and the plant output signal $y(k)$. By definition of the problem, the plant is considered causal and of non-minimum phase [1]. The IAIC structure adopted in this paper for monovariable plants was proposed by Widrow and Walach (2008) and can be seen in Figure 1.

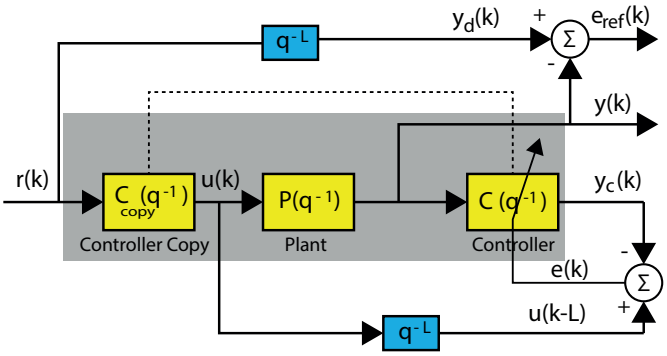

Figure 1. Block diagram for the IAIC.

The plant inverse model, i.e., the controller, is represented by $C(q^{-1})$, as can be seen. It is important to note that $C(q^{-1})$ it is equal to $C_{copy}(q^{-1})$, such that this consideration is performed in order to obtain a feedforward configuration. Furthermore, assuming that $C(q^{-1})$ is linear, then $C_{copy}(q^{-1})P(q^{-1}) \cong P(q^{-1})C(q^{-1})$ (Shafiq et al., 2017). According to Widrow and Walach (2008), ideally, $C(q^{-1})$ is considered to be equal to the plant inverse model. However, this consideration imposes limitations on the realization of IAIC, since the system is subject to uncertainty. Thus, to overcome these limitations, one alternative is to use adaptive inverse identification techniques.

In order to obtain the plant inverse model in adaptive manner, it is considered that $\hat{C}(q^{-1})$ is represented by an M-order adaptive filter of the Finite Impulse Response (FIR) type, in which $\boldsymbol{\Theta}(k) = [\theta_0\ \theta_1\ \ldots\ \theta_{M-1}] \in \mathbb{R}^{M\times 1}$ is the weights vector. Let $y_c(k)$ be the output signal of $\hat{C}(q^{-1})$, given by:

$$y_c(k) = \hat{C}(q^{-1})y(k), \qquad (2)$$

since $\hat{C}(q^{-1}) = \theta_0 + \theta_1q^{-1} + \theta_2q^{-2} + \ldots + \theta_{M-1}q^{-M}$, the output signal of $\hat{C}(q^{-1})$ is rewritten as $y_c(k) = \theta_0y(k) + \theta_1y(k-1) + \ldots + \theta_{M-1}y(k-M)$. In vectorial form (2) is rewritten as: $y_c(k) = \mathbf{Y}^T(k)\boldsymbol{\Theta}(k) = \boldsymbol{\Theta}^T(k)\mathbf{Y}(k)$, in which $\mathbf{Y}(k) = [y(k)\ y(k-1)\ \ldots\ y(k-M)] \in \mathbb{R}^{M\times 1}$ is the plant output signal vector.

[1] Since the plant is considered of non-minimum phase, therefore the plant inverse model is unstable.

To update the estimate of the weights vector $\boldsymbol{\Theta}(k)$, it is necessary to obtain the error $e(k)$. However, before obtaining $e(k)$ it is necessary to obtain the control signal, which is given by:

$$u(k) = \hat{C}_{copy}(q^{-1})r(k) \tag{3}$$

since $\hat{C}_{copy}(q^{-1}) = \theta_0 + \theta_1 q^{-1} + \theta_2 q^{-2} + \ldots + \theta_{M-1}q^{-M}$, the control signal $u(k)$ is rewritten as $u(k) = \theta_0 r(k) + \theta_1 r(k-1) + \ldots + \theta_{M-1}r(k-M)$. In vectorial form (3) is rewritten as $u(k) = \boldsymbol{\mathcal{R}}^T(k)\boldsymbol{\Theta}(k) = \boldsymbol{\Theta}^T(k)\boldsymbol{\mathcal{R}}(k)$, in which $\boldsymbol{\mathcal{R}}(k) = [r(k)\ r(k-1)\ \ldots\ r(k-M)] \in \mathbb{R}^{M\times 1}$ is reference signal vector. After obtaining the control signal $u(k)$, the error $e(k)$ is given by:

$$\begin{aligned} e(k) &= q^{-L}\hat{C}_{copy}(q^{-1})r(k) - \hat{C}(q^{-1})y(k) \\ &= q^{-L}\hat{C}_{copy}(q^{-1})r(k) - \hat{C}(q^{-1})P(q^{-1})u(k) \\ &= q^{-L}u(k) - \hat{C}(q^{-1})P(q^{-1})u(k) \\ &= \left[q^{-L} - \hat{C}(q^{-1})P(q^{-1})\right]u(k), \end{aligned} \tag{4}$$

which can be rewritten as follows:

$$e(k) = u(k-L) - [\theta_0 y(k) + \ldots + \theta_{M-1}y(k-M)] \tag{5}$$

For non-minimum phase plants, the delay block q^{-L} is important to obtain a small steady-state MSE. According to Shafiq et al. (2017), the value of L can be defined as $L \cong (\mathcal{M} + d + m)/2$, in which $\mathcal{M}$ is the generic order of an adaptive FIR filter. According to Figure 1, it is important to note that since the plant inverse dynamic is tracked by the adaptive FIR filter, $\lim_{k\to\infty}(e(k))^2 \to 0$ and, consequently, $\lim_{k\to\infty}(e_{ref}(k))^2 \to 0$.

3. DIRECT ADAPTIVE INVERSE CONTROL

The DAIC structure used in this paper for monovariable plants is shown in Figure 2 (Shafiq et al., 2017). In Figure 2, the plant inverse model, i.e., the controller, is represented by $C(q^{-1})$. Since the weights vector $C(q^{-1})$ is directly estimated, it is not necessary that the controller $C(q^{-1})$ is also cascaded to right of $P(q^{-1})$, as is used for the IAIC. Furthermore, unlike the IAIC, a strictly feedforward control configuration is not used, since the weights vector of $C(q^{-1})$ is obtained as a function of the reference error $e_{ref}(k)$.

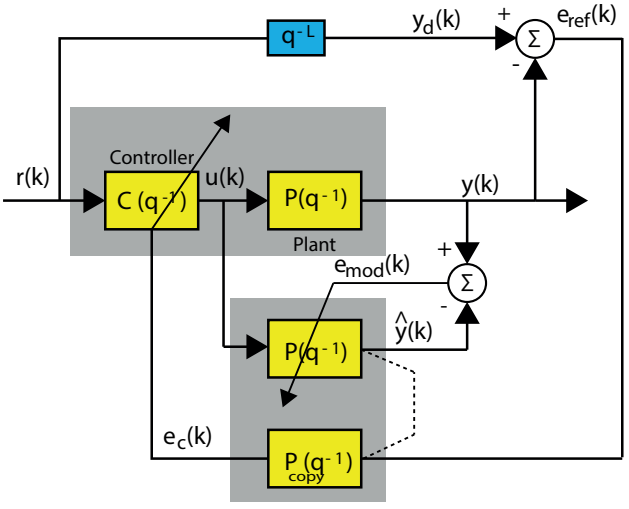

Figure 2. Block diagram for the DAIC.

Consider that the controller $\hat{C}(q^{-1})$ is represented by an M-order adaptive FIR filter, in which $\boldsymbol{\Theta}(k) = [\theta_0, \theta_1, \ldots, \theta_{M-1}] \in \mathbb{R}^{M\times 1}$ is the weights vector of $\hat{C}(q^{-1})$. Let $u(k)$ be the control signal given by:

$$u(k) = \hat{C}(q^{-1})r(k) \tag{6}$$

since $\hat{C}(q^{-1}) = \theta_0 + \theta_1 q^{-1} + \theta_2 q^{-2} + \ldots + \theta_{M-1}q^{-M}$, the control signal $u(k)$ is rewritten as $u(k) = \theta_0 r(k) + \theta_1 r(k-1) + \ldots + \theta_{M-1}r(k-M)$. In vectorial form (6) is rewritten as $u(k) = \mathbf{R}^T(k)\boldsymbol{\Theta}(k) = \boldsymbol{\Theta}^T(k)\mathbf{R}(k)$, in which $\mathbf{R}(k) = [r(k)\ r(k-1)\ \ldots\ r(k-M)] \in \mathbb{R}^{M\times 1}$ is the reference signal vector.

The error $e_c(k)$ is used to update the estimate of the weights vector $\boldsymbol{\Theta}(k)$ of $\hat{C}(q^{-1})$. However, before obtaining $e_c(k)$ it is necessary to obtain the output signal of $\hat{P}(q^{-1})$, in which $\hat{P}(q^{-1})$ is an estimate of the plant model. The model $\hat{P}(q^{-1})$ is represented by an N-order adaptive FIR filter, in which $\boldsymbol{\Pi}(k) = [\pi_0\ \pi_1\ \ldots\ \pi_{N-1}] \in \mathbb{R}^{N\times 1}$ is the weights vector. Let $\hat{y}(k)$ be the output signal of $\hat{P}(q^{-1})$ given by:

$$\hat{y}(k) = \hat{P}(q^{-1})u(k) \tag{7}$$

since $\hat{P}(q^{-1}) = \pi_0 + \pi_1 q^{-1} + \pi_2 q^{-2} + \ldots + \pi_{N-1}q^{-N}$, the output signal $\hat{y}(k)$ of $\hat{P}(q^{-1})$ is rewritten as $\hat{y}(k) = \pi_0 u(k) + \pi_1 u(k-1) + \ldots + \pi_{N-1}u(k-N)$. In vectorial form (7) is rewritten as $\hat{y}(k) = \boldsymbol{\mathcal{U}}^T(k)\boldsymbol{\Pi}(k) = \boldsymbol{\Pi}^T(k)\boldsymbol{\mathcal{U}}(k)$, in which $\boldsymbol{\mathcal{U}}(k) = [u(k)\ u(k-1)\ \ldots\ u(k-N)] \in \mathbb{R}^{N\times 1}$ is the control signal vector.

To update the estimate of the weights vector $\boldsymbol{\Pi}(k)$, it is necessary initially to obtain the estimation error $e_{mod}(k)$. Let the estimation error $e_{mod}(k)$ be given by:

$$\begin{aligned} e_{mod}(k) &= y(k) - \hat{y}(k) \\ &= P(q^{-1})u(k) - \hat{P}(q^{-1})u(k) \\ &= \left[P(q^{-1}) - \hat{P}(q^{-1})\right]u(k), \end{aligned} \tag{8}$$

in which it is can be noted that when $\hat{P}(q^{-1}) \to P(q^{-1})$, then $e_{mod}(k) \to 0$. After updating the estimate of the weights vector $\boldsymbol{\Pi}(k)$, it is obtained the error $e_c(k)$, given by:

$$e_c(k) = \hat{P}(q^{-1})e_{ref}(k), \tag{9}$$

which can be rewritten as $e_c(k) = \pi_0 e_{ref}(k) + \ldots + \pi_{N-1}e_{ref}(k-N)$, such that the reference error $e_{ref}(k)$, obtained between the reference signal $r(k)$ and the plant output signal $y(k)$, is given by:

$$\begin{aligned} e_{ref}(k) &= y_d(k) - y(k) \\ &= r(k-L) - y(k), \end{aligned} \tag{10}$$

According to Figure 2, it is important to note that since the plant inverse dynamic is tracked by the adaptive FIR, $\lim_{k\to\infty}(e_{ref}(k))^2 \to 0$ and, consequently, $\lim_{k\to\infty}(e_{mod}(k))^2 \to 0$.

4. FASS-NLMS ALGORITHM

For that the plant inverse dynamic can be tracked by the adaptive FIR filter $\hat{C}(q^{-1})$, it is necessary that the estimates of the weights vectors $\boldsymbol{\Theta}(k)$ and $\boldsymbol{\Pi}(k)$ are updated at each instant. To update the estimates of the weights vectors $\boldsymbol{\Theta}(k)$ and $\boldsymbol{\Pi}(k)$, in this paper it is used the FASS-NLMS algorithm, given below:

$$\mu(k) = \text{MFIS}(\mathcal{E}^2(k), \mathcal{K}(k))$$
$$\mathbf{\Gamma}(k+1) = \begin{cases} \mathbf{\Gamma}(k) + \mu(k)\dfrac{\mathcal{E}(k)\mathbf{\Xi}(k)}{h(k)}, & if\ h(k) \neq 0 \\ \mathbf{\Gamma}(k) & if\ h(k) = 0, \end{cases}$$
$$k \in [1, K], \tag{11}$$

in which the input variables of the antecedent of MFIS are the squared error $\mathcal{E}^2(k)$ and the normalized time instant $\mathcal{K}(k)$ by the Min-Max method. In (11), $\mu(k)$ is the adapted step size by the MFIS, $\mathbf{\Gamma}(k)$ is a generic vector which represents the weights vector $\mathbf{\Theta}(k)$ or $\mathbf{\Pi}(k)$, $\mathcal{E}^2(k)$ is a generic squared error that represents the squared error $e^2(k)$, $e_c^2(k)$ or $e_{mod}^2(k)$, $\mathbf{\Xi}(k)$ is a generic regressors vector that represents the regressors vector $\mathbf{Y}(k)$, $\mathbf{R}(k)$ or $\boldsymbol{\mathcal{U}}(k)$, $h(k) = \mathbf{\Xi}^T(k)\mathbf{\Xi}(k)$, $\mathcal{K}(k)$ is the normalized time instant by the Min-Max method, and K is the total number of time instants.

$$\begin{aligned}
\mathcal{R}^1 &: \textbf{If } \mathcal{K}(k) \textit{ is } S \textbf{ and } \mathcal{E}^2(k) \textit{ is } S \textbf{ then } \bar{\mu}(k) \textit{ is } M \\
\mathcal{R}^2 &: \textbf{If } \mathcal{K}(k) \textit{ is } S \textbf{ and } \mathcal{E}^2(k) \textit{ is } M \textbf{ then } \bar{\mu}(k) \textit{ is } M \\
\mathcal{R}^3 &: \textbf{If } \mathcal{K}(k) \textit{ is } S \textbf{ and } \mathcal{E}^2(k) \textit{ is } L \textbf{ then } \bar{\mu}(k) \textit{ is } M \\
\mathcal{R}^4 &: \textbf{If } \mathcal{K}(k) \textit{ is } M \textbf{ and } \mathcal{E}^2(k) \textit{ is } S \textbf{ then } \bar{\mu}(k) \textit{ is } S \\
\mathcal{R}^5 &: \textbf{If } \mathcal{K}(k) \textit{ is } M \textbf{ and } \mathcal{E}^2(k) \textit{ is } M \textbf{ then } \bar{\mu}(k) \textit{ is } S \\
\mathcal{R}^6 &: \textbf{If } \mathcal{K}(k) \textit{ is } M \textbf{ and } \mathcal{E}^2(k) \textit{ is } L \textbf{ then } \bar{\mu}(k) \textit{ is } L \\
\mathcal{R}^7 &: \textbf{If } \mathcal{K}(k) \textit{ is } L \textbf{ and } \mathcal{E}^2(k) \textit{ is } S \textbf{ then } \bar{\mu}(k) \textit{ is } S \\
\mathcal{R}^8 &: \textbf{If } \mathcal{K}(k) \textit{ is } L \textbf{ and } \mathcal{E}^2(k) \textit{ is } M \textbf{ then } \bar{\mu}(k) \textit{ is } M \\
\mathcal{R}^9 &: \textbf{If } \mathcal{K}(k) \textit{ is } L \textbf{ and } \mathcal{E}^2(k) \textit{ is } L \textbf{ then } \bar{\mu}(k) \textit{ is } L
\end{aligned} \tag{12}$$

The input variables of MFIS are the linguistic variables of the antecedent. Each linguistic variable of the antecedent, through the fuzzification, receives each linguistic value of the antecedent with a membership degree that belongs to the interval $[0, 1]$. This operation is performed through the following mappings $m_j(\mathcal{K}(k)) : U \to [0, 1]$ and $m_j(\mathcal{E}^2(k)) : V \to [0, 1]$, with the universes of discourse $U = [0, 1]$ and $V = [0.1 \times 10^{-5}, 3 \times 10^{-5}]$. It is important to note that each linguistic value is defined by a Membership Function (MBF) which characterizes a fuzzy set. The mapping is performed through the j-th MBF $m_j(\bullet)$ of each linguistic variable of the antecedent. According to the expert's knowledge, three MBFs of triangular type were defined for each linguistic variable of the antecedent, with the linguistic values small (S) for $j = 1$, medium (M) for $j = 2$ and large (L) for $j = 3$, as can be seen in Figures 3a and 3b.

With respect to the consequent of MFIS, the linguistic variable of the consequent $\bar{\mu}(k)$ receives each linguistic value of the consequent with a membership degree that belongs to the interval $[0, 1]$, through the following mapping $m_j(\bar{\mu}(k)) : Z \to [0, 1]$, with the universe of discourse $Z = [0, 0.1]$. According to the expert's knowledge, three MBFs of triangular type were defined for each linguistic variable of the consequent, with the linguistic values small (S) for $j = 1$, medium (M) for $j = 2$ and large (L) for $j = 3$, as can be seen in Figure 3c.

In (12), the rule base developed for adaptation of the step size $\mu(k)$ is presented. Due to the step size be adapted by an MFIS, the parameters of MBFs and of the rule base were defined according to the expert's knowledge about how the trade-off between the convergence speed

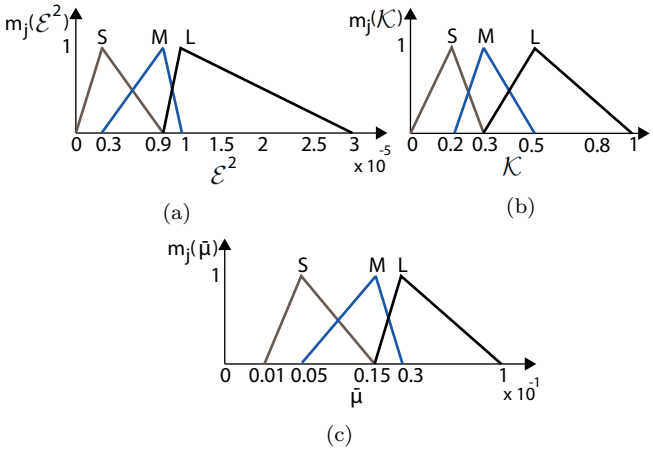

Figure 3. MBFs, (a) Linguistic variable $\mathcal{E}(k)$, (b) Linguistic variable $\mathcal{K}(k)$ and (c) Linguistic variable $\bar{\mu}(k)$.

and the steady-state MSE should be realized. The expert's knowledge can be obtained,for example, through past experiences of the analyzed problem. The fuzzy propositions of the antecedent and consequent presented in the rule base are related through a conditional fuzzy proposition. The conditional fuzzy proposition is characterized by the fuzzy implication of the universes of discourse of the antecedent for the universe of discourse of the consequent, such that the input of the fuzzy implication is the degree of activation of each fuzzy rule characterized by the t-norm of MBFs of the antecedent, given by:

$$\alpha^i = m(\mathcal{K}(k), \mathcal{E}^2(k)) = \min[m_j(\mathcal{K}(k)), m_j(\mathcal{E}^2(k))] \tag{13}$$

and the output of the fuzzy implication is an MBF given by:

$$m_{\mathcal{R}^i} = \min[\alpha^i, m_j(\bar{\mu}(k))] \tag{14}$$

Since each fuzzy rule is activated with a certain degree of activation, then the fuzzy implication is performed for each fuzzy rule and, consequently, for each fuzzy rule is obtained an MBF given in (14). In order to combine all the MBFs $m_{\mathcal{R}^i}$ with $i = 1, 2, \ldots, 9$, aiming to obtain a single MBF that represents the total response of MFIS due to performing of the fuzzy implication, it is performed the fuzzy aggregation. Through the fuzzy aggregation, all MBFs $m_{\mathcal{R}^i}$ are combined as follows:

$$m_{Total} = \max[m_{\mathcal{R}^1}, m_{\mathcal{R}^2}, \ldots, m_{\mathcal{R}^9}] \tag{15}$$

After performed the fuzzy aggregation , it is necessary that m_{Total} be defuzzified so that the step size $\mu(k)$ received a numerical value. In this work, the defuzzification method used is of centroid type, given by:

$$\mu(k) = \frac{\sum_{i=1}^{9} \bar{\mu}^i(k) m_{Total}(\bar{\mu}^i(k))}{\sum_{i=1}^{9} m_{Total}(\bar{\mu}^i(k))} \tag{16}$$

5. COMPUTATIONAL RESULTS

In this section are presented the results obtained by the applying of DAIC and IAIC to an Electro-Hydraulic (EHA) system. EHA systems are widely used in engineering, due to their high power-weight ratio, their ability to deliver high force intensity and their compact size. The researchers are increasingly interested in developing and applying control methodologies for positioning in EHA systems. Therefore, it becomes interesting to use a DAIC and IAIC

for the control of an EHA system. The model of the EHA system used in this section to represent the plant $P(q^{-1})$ was obtained experimentally in Ghazali et al. (2015), given by:

$$y(k) = \frac{-0.03093 + 0.3836q^{-1} - 0.2738q^{-2}}{1 - 1.57q^{-1} + 1.056q^{-2} - 0.1695q^{-3}}(u(k) + n(k)), \tag{17}$$

in which $n(k)$ (V) is the periodic disturbance signal added to the control signal $u(k)$ (V) and $y(k)$ (mm) is the piston displacement of the EHA system or plant output signal.

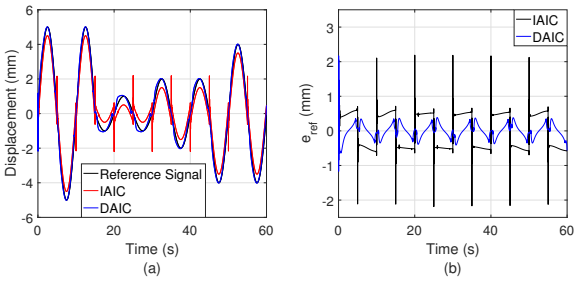

Figure 4. Plant output signal $y(k)$ (a) and Reference error $e_{ref}(k)$ (b).

The plant $P(q^{-1})$ is of non-minimum phase and stable, with zeros located at 11.6418 and 0.7604, and with poles located at $0.6725 \pm 0.5488i$ and 0.2250. To explore the tracking ability of the plant inverse dynamic and, consequently, of the reference signal, a sinusoidal signal with frequency $f = 0.1$Hz was defined as the reference signal $r(k)$, given by:

$$r(k) = \begin{cases} 5sin(\omega t), & \text{if} \quad 1 \leq k \leq 3000 \\ 1sin(\omega t), & \text{if} \quad 3001 \leq k \leq 6000 \\ 2sin(\omega t), & \text{if} \quad 6001 \leq k \leq 9000 \\ 4sin(\omega t), & \text{if} \quad 9001 \leq k \leq 12000, \end{cases} \tag{18}$$

in which $t = T_a k$ and $\omega = 2\pi f$. The total time of simulation was set equal to 60 s, in which the sampling period used was set equal to $T_a = 5$ ms and the total number of time instants was set equal to $K = 12000$. The objective of using a sinusoidal signal as the reference signal for an EHA system, is that through it a velocity range is generated from zero to the maximum attainable value in each direction where the highest friction occurs during the low speed condition and when reversing the actuator move in the EHA system Ghazali et al. (2015). Thus, using a sinusoidal signal as the reference signal is a challenge for the control of EHA systems.

$$n(k) = \begin{cases} -2, & \text{if} \quad 1 \leq k \leq 2000 \\ 2, & \text{if} \quad 2001 \leq k \leq 3000 \\ -2, & \text{if} \quad 3001 \leq k \leq 4000 \\ 2, & \text{if} \quad 4001 \leq k \leq 5000 \\ -2, & \text{if} \quad 5001 \leq k \leq 6000 \\ 2, & \text{if} \quad 6001 \leq k \leq 7000 \\ -2, & \text{if} \quad 7001 \leq k \leq 8000 \\ 2, & \text{if} \quad 8001 \leq k \leq 9000 \\ -2, & \text{if} \quad 9001 \leq k \leq 10000 \\ 2, & \text{if} \quad 10001 \leq k \leq 11000 \\ -2, & \text{if} \quad 11001 \leq k \leq 12000 \end{cases} \tag{19}$$

The order of adaptive FIR filters $\hat{C}(q^{-1})$ and $\hat{P}_{copy}(q^{-1}) = \hat{P}(q^{-1})$ for the DAIC and IAIC was set equal to $M = N = 10$. The delay block q^{-L} was set equal to $L = 6$. The performance analysis of trade-off for the FASS-NLMS algorithm was performed only with respect to $\hat{C}(q^{-1})$, in which the convergence speed of the weights vector $\mathbf{\Theta}(k)$ can be verified, for example, through the convergence speed of the plant output signal $y(k)$ to the reference signal $r(k)$ and, the steady-state MSE can be verified through MSE of $e_c(k)$ (used to update the estimate of the weights vector $\mathbf{\Theta}(k)$ for the DAIC) and through MSE of $e(k)$ (used to update the estimate of the weights vector $\mathbf{\Theta}(k)$ for the IAIC).

The periodic disturbance signal was set equal to (19). The tracking of the reference signal $r(k)$ developed by the DAIC and IAIC designed by the FASS-NLMS algorithm is shown in Figure 4 (a). For the DAIC, the satisfactory tracking of the plant inverse dynamic and, consequently, of the reference signal $r(k)$, even in the presence of the periodic disturbance signal $n(k)$, was possible due to estimate of the weights vector $\mathbf{\Theta}(k)$ of $\hat{C}(q^{-1})$ be performed as a function of the reference error $e_{ref}(k)$ and of the estimation error $e_{mod}(k)$ of $\hat{P}(q^{-1})$. For the IAIC, since it is implemented in a strictly feedforward configuration, the update of the estimate of the weights vector $\mathbf{\Theta}(k)$ is not performed as a function of the reference error $e_{ref}(k)$; thus, the tracking performance of the plant inverse dynamic and, consequently, of the reference signal $r(k)$ was unsatisfactory, as shown in Figure 4 (a). Furthermore, in Figure 4 (a) it is observed that the plant output signal $y(k)$ for the DAIC, when compared to the IAIC, obtained a higher convergence speed to the reference signal $r(k)$. These affirmations can also be verified through the reference error $e_{ref}(k)$ shown in Figure 4 (b), where it is observed that the plant output signal $y(k)$ for the DAIC obtained a satisfactory performance in the tracking of the reference signal $r(k)$, when compared to the IAIC.

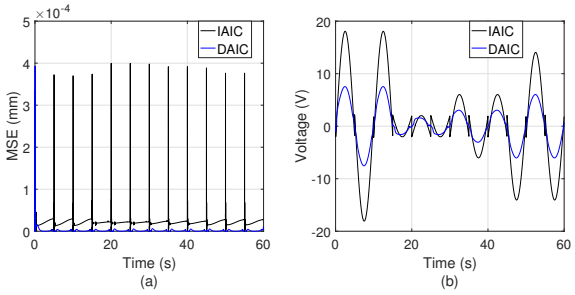

Figure 5. MSE of $e(k)$ (black color) and MSE of $e_c(k)$ (blue color) (a) and Control signal $u(k)$ (b).

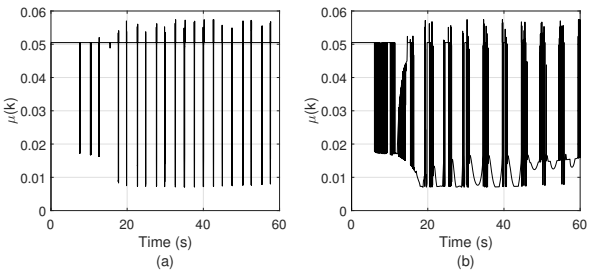

Figure 6. Step Size for the DAIC (a) and Step Size for the IAIC (b).

Since the errors $e_c(k)$ and $e(k)$ are used to update the estimate of the weights vector $\mathbf{\Theta}(k)$ for the DAIC and IAIC, in Figure 5 (a) is shown the MSE of $e_c(k)$ and $e(k)$. For the DAIC, the MSE of $e_c(k)$ confirms the tracking ability of the plant inverse dynamic and, consequently, of the reference signal $r(k)$, in which the steady-state MSE quickly tend to zero and with a small amplitude at each change of amplitude of the reference signal $r(k)$. In Figure 5 (b) is shown the control signal $u(k)$ developed by the DAIC and IAIC. It is noted that the control signal $u(k)$ developed by the IAIC obtained higher amplitudes than the control signal $u(k)$ developed by the DAIC. Due to the unsatisfactory performance of the IAIC, it is noted that the parametric adaptation of the step size for update of the estimate of the weights vector $\mathbf{\Theta}(k)$ of $\hat{C}(q^{-1})$, obtained intense variations during its time evolution, as shown in Figure 6 (b).

In Figure 6 (a) is show the time evolution of the adaptation of the step size for update of the estimate of the weights vector $\mathbf{\Theta}(k)$ of $\hat{C}(q^{-1})$ for the DAIC. During the parametric adaptation of the step size for the DAIC, even after the amplitude change of the periodic disturbance signal $n(k)$, were obtained less intense variations when compared to the IAIC, which is result of its higher disturbance rejection ability.

6. CONCLUSION

In this paper, the step size of NLMS algorithm is adapted by an MFIS, with the objective of obtain a good trade-off between the convergence speed and the steady-state MSE. The proposed optimization algorithm was applied to DAIC and IAIC design for a non-minimum phase EHA system in the presence of a periodic disturbance signal added to the control signal. In the results obtained, it was possible to observe the good performance of the proposed optimization algorithm, with respect to the convergence speed and to the steady-state MSE. It was observed that, due to adaptation of the step size through MFIS, even after the amplitude change of the periodic disturbance signal, the plant output signal for the DAIC still continued to converge to the reference signal, exhibiting a behavior of disturbances rejecting. Also with regard to MFIS, it can be seen that the step size is adapted independently of high-order statistical measures.

REFERENCES

Benesty, J., Rey, H., Vega, L.R., and Tressens, S. (2006). A nonparametric vss nlms algorithm. *IEEE Signal Processing Letters*, 13(10), 581–584.

Bershad, N.J. and Bermudez, J.C. (2020). A switched variable step size nlms adaptive filter. *Digital Signal Processing*, 101, 102730.

Dhimish, M., Holmes, V., Mehrdadi, B., and Dales, M. (2018). Comparing mamdani sugeno fuzzy logic and rbf ann network for pv fault detection. *Renewable energy*, 117, 257–274.

Farhang-Boroujeny, B. (2013). *Adaptive filters: theory and applications*. John Wiley & Sons.

Ghazali, R., Sam, Y.M., Rahmat, M., Soon, C., Jaafar, H., et al. (2015). Discrete sliding mode control for a non-minimum phase electro-hydraulic actuator system. In *2015 10th Asian Control Conference (ASCC)*, 1–6. IEEE.

Kamanditya, B. and Kusumoputro, B. (2020). Elman recurrent neural networks based direct inverse control for quadrotor attitude and altitude control. In *2020 International Conference on Intelligent Engineering and Management (ICIEM)*, 39–43. IEEE.

Kim, D.W., Hur, J., and Park, P. (2020). Two-stage active noise control with online secondary-path filter based on an adapted scheduled-stepsize nlms algorithm. *Applied Acoustics*, 158, 107031.

Li, X., Zhao, T., Fan, P., and Zhang, J. (2019). Rule-based fuzzy control method for static pressure reset using improved mamdani model in vav systems. *Journal of Building Engineering*, 22, 192–199.

Ng, Y., Mohamad, H., and Chuah, T. (2009). Block-based fuzzy step size nlms algorithms for subband adaptive channel equalisation. *IET Signal Processing*, 3(1), 23–32.

Pauline, S.H., Samiappan, D., Kumar, R., Anand, A., and Kar, A. (2020). Variable tap-length non-parametric variable step-size nlms adaptive filtering algorithm for acoustic echo cancellation. *Applied Acoustics*, 159, 107074.

Resende, L.C., Haddad, D.B., and Petraglia, M.R. (2018). A variable step-size nlms algorithm with adaptive coefficient vector reusing. In *2018 IEEE International Conference on Electro/Information Technology (EIT)*, 0181–0186. IEEE.

Shafiq, M., Shafiq, M.A., and Yousef, H.A. (2017). Stability and convergence analysis of direct adaptive inverse control. *Complexity*, 2017.

Shafiq, M.A. (2016). Direct adaptive inverse control of nonlinear plants using neural networks. In *2016 Future Technologies Conference (FTC)*, 827–830. IEEE.

Shafiq, M.A., Shafiq, M., and Ahmed, N. (2014). Closed loop direct adaptive inverse control for linear plants. *The Scientific World Journal*, 2014.

Wang, X.Y., Wang, Y., and Li, Z.S. (2013). Research of the 3-dof helicopter system based on adaptive inverse control. In *Applied Mechanics and Materials*, volume 389, 623–631. Trans Tech Publ.

Widrow, B. and Walach, E. (1983). Adaptive signal processing for adaptive control. *IFAC Proceedings Volumes*, 16(9), 7–12.

Widrow, B. and Walach, E. (2008). Adaptive inverse control: A signal processing approach, reissue ed.

Zhang, G., Wang, Y., Fan, Y., and Chen, C. (2018). Adaptive inverse control based on kriging algorithm and lyapunov theory of crawler electromechanical system. *Complexity*, 2018.